

# Rethinking the Complexity and Uncertainty of Spatial Networks Applied to Forest Ecology

Hao-Ran Wu

Zhejiang University

Chen Peng

Zhejiang University

Ming Chen (✉ [mchen@zju.edu.cn](mailto:mchen@zju.edu.cn))

Zhejiang University

---

## Article

## Keywords:

**Posted Date:** March 11th, 2022

**DOI:** <https://doi.org/10.21203/rs.3.rs-1431142/v1>

**License:**  This work is licensed under a Creative Commons Attribution 4.0 International License.

[Read Full License](#)

---

# Abstract

Characterizing tree spatial patterns and interactions are helpful to reveal underlying processes assembling forest communities. Spatial networks, despite its complexity, are powerful to examine spatial interactions at an individual level using well defined patterns. However, complex tree networks introduce uncertainties. Validation methods are needed in order to assess whether network-based metrics can clearly identify different processes. Here, we constructed three types of tree networks, which reflect various aspects of tree competition. Based on five types of spatial null models and 199 Monte-Carlo simulations, we were able to select network-based metrics that exhibited well performances on distinguishing different processes. This technique was then applied to forest dataset Tuscany of Italy. We found that the average node degree and the cluster coefficient are ideal metrics like the Ripley's K and paired correlation function. In addition, network approach can identify fine-scale spatial variations of tree competition and its underlying causes. Our analyzes also indicate that a bit of caution is needed when defining the network structure as well as designing network-based metrics. We suggested that validation techniques using corresponding spatial null models are critically important to reduce the negative effects caused by uncertainties of the network.

## Introduction

Forest plays an important role in global carbon cycle<sup>1,2</sup>, biodiversity maintenance<sup>3</sup>, and human well-being<sup>4</sup>. Despite the critical values of forests to help mitigate human-caused climate change, climate-driven risks<sup>5</sup> as well as habitat fragmentation<sup>6,7</sup> have proposed a threat to forest stability. Due to the rapid deforestation in the past decades, forest restoration has been regarded as a priority at the global scale<sup>8</sup>. Clear understanding and quantification of mechanisms assembling forest communities are likely to have substantial benefits for forest restoration and biological conservation<sup>9-11</sup>.

Various processes—ranging from environmental filtering, dispersal limitation and competition to disturbance—have an impact on forest structure<sup>12</sup>. Successful colonization of a particular sites relies on the capacity to overcome environmental and biotic barriers<sup>13</sup>. The latter includes species interactions like competition and the Janzen–Connell (JC) effects<sup>14,15</sup>, which is closely related to the structure and dynamics of the forest community<sup>16</sup>. Inter-tree competition for resources (i.e. light, space, and nutrient) may be prevalent<sup>16,17</sup>. However, due to its spatial complexity, processes altering tree interactions are still poorly understood. One of the mechanisms that increase density-dependent tree mortality is dispersal limitation<sup>18</sup>. Seeds fail to reach remote sites may undergo higher level of competition<sup>19</sup>. Other processes like fire exclusion<sup>20</sup>, wind disturbance<sup>21</sup>, and flooding<sup>22</sup> may reduce tree competition, thus alter the mortality patterns and spatial arrangement of tree interactions. Studies have shown that higher tree densities did not necessarily translate into increased mortality<sup>23</sup>. In seedling stage, facilitation across individuals is prevalent. Strong competition is usually detected in adult trees<sup>17,24,25</sup>. Closed phylogenetic relationships can also lead to higher level of competition<sup>24</sup>. Thus, techniques are needed to decompose spatial variations of tree interactions and reveal its underlying mechanisms.

During the past decades, interest in methods for analyzing spatial dataset expanded rapidly in ecology<sup>26-29</sup>. It is critical for evaluating ecological theories<sup>30</sup>. Existing spatially explicit metrics applied to community ecology ranges from spatial point pattern analysis and quadrat-based analyses to individual-based neighborhood models, which are powerful to reveal spatial processes in fully mapped communities at several scales simultaneously<sup>29</sup>. For spatial variations of tree interactions, the limitation of such analyses lays in the assumption that tree competes for space, regardless of light and nutrients. Also, local spatial variations are usually ignored in these metrics. For example, many summary statistics derived from the Ripley's  $K$  statistic<sup>31</sup> count for averaged spatial crowdedness within a specific region. To quantify clumping, these measures implicitly assume homogeneous intensity of point process<sup>26,27</sup>. Nearest-neighbor statistics<sup>29,32-34</sup> identify spatial clusters using nearest distance approaches. Despite its powerfulness, many ecological processes, such as habitat filtering, can be better revealed by identifying the spatial position of each cluster<sup>30</sup>.

Ecological networks, despite its complexity, are powerful to reveal ecological mechanisms using well defined patterns<sup>35-37</sup>. Network systems usually include nodes (i.e. units of biological hierarchy) and edges (i.e. interactions between nodes), which defines complex network structure of ecological systems rather than pairwise interactions<sup>38</sup>. Mathematical approaches, including the analysis of graph-theoretical properties, can be applied to examine interactions among large numbers of nodes efficiently<sup>38,39</sup>. In plant ecology, networks are used to characterize individual-level interactions such as competition, facilitation, and predation<sup>16,35,36,39</sup>. By introducing binary and weighted out-degrees, Nakagawa et al.<sup>39</sup> found that larger plants competed more strongly with other large plants in 1948, but they competed preferentially with small plants after 30 years in Hokkaido, Japan. By constructing tree networks, Schmid et al.<sup>16</sup> found that pioneer species were not tend to be shaded by other trees. Despite its powerfulness to reveal additional ecological information, complex tree competition networks introduce uncertainties. Attempts should be made to validate the relatedness between network-based spatial explicit metrics and underlying processes.

In this article we develop an approach to characterize spatial distribution of individual-level tree interactions based on network approaches (Fig. 1). We construct three types of tree networks to characterize tree competitions for light and space. Using several spatial null models with different ecological hypotheses, we validate network-based spatially explicit metrics (i.e. average node degree, average path length, density, clustering coefficient) by Monte-Carlo simulations. For each spatially explicit metrics, ranging from network-based metrics, to Ripley's  $K$  and pair correlation function (PCF) function  $g(r)$ , we compare the ability of each metrics to characterize tree spatial patterns and interactions, and the ability to reveal underlying processes. To test the effectiveness of our network-based metrics, we further applied this technique to real forest dataset in Tuscany (central Italy) to investigate the intensity and spatial distribution of tree competition. We conclude by discussing the advantages of network approached applied to spatial ecology as well as some cautions need to be considered for the design and validation of the spatially explicit metrics in general.

# Results

## Network characteristics of tree competition

For each spatial null model, we constructed three types of tree networks (Fig. 2). 199 Monte-Carlo simulations were performed for each type of null model. A total of 1,990 undirected tree networks (CS and CL) and 995 bi-directed tree networks (WCL) were constructed. We founded that tree networks based on cluster models were highly connected. In CL, for example, 3101.29 edges were presented in networks based on Thomas process on average (ranged from 1788–4164), followed by Matérn process (2891.74 on average, ranged from 1920–4060), CSR (1383.14 on average, ranged from 1114–1762), Strass process (673.97 on average, ranged from 528–858), and HC (358.05 on average, ranged from 280–480).

Both average node degree  $k$  and clustering coefficient  $C$  showed a distinctive difference among five processes in unweighted networks (Fig. 3; See supplementary Table S1 for details). In CL, average  $k$  in Thomas process was highest (5.31 on average, ranged from 3.95–6.41), significantly larger than that in CSR (2.61 on average, ranged from 2.28–3.00), Strass process (1.92 on average, ranged from 1.70–2.16), and HC (1.54 on average, ranged from 1.33–1.81) (Fig. 3B). Similarly,  $k$  value was significantly higher in cluster processes in CS network (Fig. 3A). No overlapping ranges of  $k$  value among cluster processes, CSR, and Gibbs processes were detected in both CS and CL networks (Fig. 3A, B). Average  $C$  distribution showed similarities to  $k$  value despite minor overlapping ranges. In CL, average  $C$  in Thomas process was (0.83 on average, ranged from 0.78–0.89), much higher than that in CSR (0.57 on average, ranged from 0.49–0.63), Strass process (0.47 on average, ranged from 0.39–0.54), and HC (0.31 on average, 0.15–0.31) (Fig. 3A).

In WCL, nevertheless, average weighted  $k$  value distribution only showed small differences among various models (Fig. 3C). Overlapping of weighted  $k$  value in five models ranged from 1.36–82.81. The density  $D$  and the average path length  $L$  of the network failed to distinguish most types of the models. In CS, for instance, no significant differences were found between  $D$  value in CSR (0.0077 on average, ranged from 0.0070–0.0084) and that in HC (0.0075 on average, ranged from 0.0067–0.0087) (Fig. 3A). Overlapping of  $D$  value among various models were frequent in CS and CL (Fig. 3A, B). For  $L$  value, huge variance and many outliers within each model was found, leading to its poor ability to distinguish different types of the models (Fig. 3).

The results of node degree distribution in various models are shown in Fig. 4. In CS, 97.75%, 92.91%, and 64.46% nodes were connected with less than 12 other nodes on average in HC, Strass process, and CSR, respectively (Fig. 4A). A similar pattern was found in CL (Fig. 3B). For cluster processes, variation of node degree was significantly larger than that in CSR and Gibbs processes. The peak value of probability density in cluster models was much lower (Fig. 4A, B). On the contrary, no significant differences were found for both node degree and edge weight distribution in WCL (Fig. 4C, D).

## Spatial patterns of tree interactions

Based on 199 Monte-Carlo simulations, the univariate  $K(r)$  function showed different patterns among various spatial null models (Fig. 5). At scales  $r < 15\text{m}$ , the lower bound of the envelope generated by Thomas process was higher than the upper bound of that by CSR. Similarly, envelope generated by CSR exhibited higher values than that by HC at short distances,  $r < 10\text{m}$ . When the scales become larger, overlaps were detected between different envelopes. Envelopes calculated by  $g(r)$  showed similarities to that by  $K(r)$ . At scales  $r < 5\text{m}$ , envelope by Thomas process showed the highest values, followed by CSR and HC. Again, overlaps occurred when scales became larger.

### Spatial variations of network characteristics

We found that average node degree  $k$  showed distinctive distribution patterns among different spatial models (Supplementary Fig. S1). Cluster processes exhibit high levels of spatial inhomogeneity. The spatial distributions of  $k$  value in Gibbs processes showed a smooth trend with low values at most regions. Betweenness centrality in CSR was generally much higher compared to that in cluster and Gibbs processes.

### Application of network-based metrics to Tuscany

We applied four types of network-based metrics to forest plots in Tuscany (Table 1). CS, CL, and WCL networks were constructed based on field investigation dataset in Tuscany (Fig. 6A). In CS, the value of average node degree  $k$  located within the region generated by CSR, while the value of clustering coefficient  $C$  located at the transition zone between HC and Strass process. The pattern was similar in CL. Distributions of  $k$  and betweenness centrality of each node in tree networks were shown in Fig. 6B.

Table 1

Network metrics of the Tuscany dataset. Indices in the table includes: n.nodes – the number of nodes, n.edges – the number of edges,  $k$  – the average node degree,  $D$  – the density of the network,  $L$  – the average path length. The value of  $C, D, L$  in WCL is identical to CL due to the same definition of tree network except edge weight.

	n.nodes	n.edges	k	C	D	L
CS	2119	9250	4.365267	0.486646	0.002061	7.749475
CL	1999	6122	3.062531	0.386719	0.001533	8.443343
WCL	1999	6122	0.782276	/	/	/

## Discussion

Both node degree and clustering coefficient seem to be ideal spatial explicit metrics to examine tree spatial patterns. We found that average node degree  $k$  showed a distinctive pattern without any overlap ranges among cluster processes, CSR, and Gibbs processes. Average clustering coefficient  $C$  also showed its ability to characterize different processes in specific ranges despite some minor overlaps (Fig. 3). According to the definitions of the cluster processes, a set of ‘parent’ points is randomly generated before

each of them gives rise to a random pattern of 'offspring' points within a disc and dies<sup>26,40</sup>. Nodes in the networks are hence more likely to find close neighbors within a short distance, leading to higher a node degree. Clustering coefficient  $C$  analyzed local density of the network. 'offspring' points generated by cluster models tend to be closer compare to points generate by CSR, thus the division of the number of connected edges by maximum possible edges within local network is higher.

Despite of their excellent performance in distinguishing various processes, average node degree  $k$  and cluster coefficient  $C$  showed different degree of variations. For cluster models, huge variation of average node degree was found (Fig. 3A, B). One of the reasons might be variations of paired distance between clusters. Since 'parent' points are generated according to CSR, the clusters are randomly distributed. Isolated clusters can lead to low values of  $k$ . However, clustering coefficient calculates the number of connected edges between the neighbors of nodes<sup>16</sup>, thus diminishes the effects of cluster distance. We also found little variation of  $k$  value in Gibbs models (Fig. 3A, B). In Gibbs process, strong interactions (represented by closed distance) between trees are not allowed. Hence a uniformly distributed pattern would be generated<sup>26</sup>, which might reduce the variations of the number of neighbors. Consequently, we advised that average node degree  $k$  is plausible to identify regular patterns while cluster coefficient  $C$  is an ideal metrics to examine aggregated patterns.

Node degree distributions of the networks followed heavy-tailed distributions, similar to a wide range of previous studies in forest ecology based on network approaches<sup>16,35,39</sup>. Particularly, node degrees in cluster models were highly variable (Fig. 4A, B). Again, we suspected that it is caused by the uncertainty of paired distance between clusters. Isolated clusters tend to have fewer neighbors, leading to lower node degree. Mechanisms of Gibbs process and CSR are similar expect that the former deletes realizations that contain two points within a threshold distance<sup>26</sup>. Consequently, the shapes of node degree distribution curve showed similarities between among HC, Strass process, and CSR. The only difference was that node degrees were generally lower in HC and Strass process, compared to that in CSR.

Unfortunately, the density  $D$  and the average path length  $L$  of the network fail to distinguish the spatial models. Average path length  $L$  is a measure of global connectivity or spatial segregation of the network<sup>16,35,41</sup>. It calculates the shortest distance between two connected nodes, quantified by the number of edges between them<sup>35</sup>. According to the definition of CL and CS networks, two nodes are connected only if there are enough points or overlapping tree crowns between them, which introduces uncertainties to the calculation of  $L$  value. The same might also be true for density  $D$ .

By applying network-based metrics to real plantation dataset in Tuscany, our findings revealed regular and random distribution patterns, which indicates low intensity of tree competition (Table 1; Fig. 3). Currently, most plantations are established with one tree on each planting point. Pairwise distance between planting points is often constant, resulting in regular patterns<sup>42</sup>, which is detected by our network approach.

Network-based metrics is a powerful way to analyze complex interactions in forests<sup>16</sup>. Like the Ripley's  $K$  and  $g(r)$  (Fig. 5), we found that network characteristics such as average node degree  $k$  and cluster coefficient  $C$  exhibited excellent performance in examining underlying processes, at least at small scales (Fig. 3). In addition, network-based metrics are highly flexible in order to examine complex tree interactions<sup>36</sup>. Network approaches can also help to reveal additional information of forest structures. Based on spline interpolation, attempts can be made to infer the regions with high competition values. Betweenness centrality has been applied in previous studies to identify the populations that have a huge impact on gene flow<sup>43</sup>. In this study, we found regions that largely affected the overall structure of competition networks indicated by high values of betweenness centrality (Fig. 6B and Supplementary Fig. S1). Management implications can be selective loggings on trees with high centrality scores for regeneration and seedling survival.

Nevertheless, a bit of caution is needed when designing the network-based spatial explicit metrics. Ecology networks are highly complex, with their general patterns and underlying causes still debated<sup>37</sup>. Network and graph theory provide a flexible conceptual model that can help identify the relationship between complex structures and processes<sup>44</sup>. Additional information like numerous competition kernel functions were applied in previous studies<sup>39</sup>. We cautioned that, however, introducing network-based metrics may increase the uncertainty and thus reducing its ability to identify underlying processes. In this study, we found that all of the network characteristics failed to distinguish different spatial processes in WCL (Fig. 3C). Neither weighted node degree distribution nor edge length distribution showed differences among various types of the spatial models (Fig. 4C, D). We provided three possible explanations for this: (1) For each pair of the nodes in bi-directed WCL, a high  $C$  value from Tree-1 to Tree-2 is corresponding to a low  $C$  value from Tree-2 to Tree-1. Hence the counteracting effects may occur for each pair of the  $C$  values; (2) The  $C$  value increases disproportionately with the decreasing distance, which adds uncertainty in the calculation of weighted node degree; (3) A fractional formula, despite its popularity in the design of competition index, may amplify the effects of crown sizes on the competition intensity of trees and, consequently, aggregated patterns are not necessarily translated into higher intensity of competition. We then suggested that trade-offs between complexity and uncertainty as well as a deeper understanding of tree competitions are important when designing network-based spatial explicit metrics.

Spatial network is a powerful tool to reveal ecological complexity and underlying processes<sup>16,35,36</sup>. Network approaches can examine fine-scale spatial distribution, connectivity, and intensity of tree interactions using a combination of geographic and crown size datasets. Network-based spatial metrics prompts us to rethink previous spatial explicit metrics (i.e. Ripley's  $K$ , Nearest-neighborhood approach, etc.)<sup>29</sup>. However, validations of network-based metrics were often ignored in previous studies. We advised a workflow (Fig. 1) to characterizing tree spatial patterns and interactions using network approaches: (1) Collect data by remote sensing techniques; (2) Tree crown segmentation and validation; (3) Construct the network and define the weight; (4) Validate the network using spatial null models; (5) If accepted, the expression of weight can be applied to a specific research. We also provided spatio-temporal datasets in various forests based on UAV. The dataset is available at BioRS (<http://bis.zju.edu.cn/biors>).

Overall, the current study described the tree spatial patterns and interactions using three types of networks, namely competition for space (CS), competition for light (CL), and weighted competition for light (WCL). We applied four types of network-based metrics to detected underlying ecological processes using five hypothetic models: (1) CSR, (2) Matérn process, (3) Thomas process, (4) HC, (5) Strass process. We concluded that: (1) Both node degree distribution and clustering coefficient are ideal metrics in CS and CL networks to distinguish multiple processes, (2) Network approaches are powerful tools to describe fine-scale spatial variations of tree interactions. They can also help identify units that have a large impact on the overall structure of the network and thus giving management implications, (3) Despite its complexity, an important precaution for reducing the uncertainties of the network is careful validation using corresponding spatial null models.

## Methods

### Dataset collection

We selected real forest dataset from field investigations. The dataset provides an exhaustive tree inventory with forest mensuration and spatial location carried out in 54 plots sampled in 45- to 55-year-old black pine plantations, located in two areas of Tuscany, Italy<sup>45</sup>. Forest mensuration includes diameters at breast height, total height of the tree, crown depth, etc. A total of 4171 trees were mapped in the dataset. The data was collected during the last quarter of 2014. We chose zone 1 (Monte Amiata) data to construct network, which included 2166 trees, and summary statistics of the collected data before the treatment are reported in Table 2.

Table 2  
Main descriptive statistics of collected data in zone 1, Tuscany, Italy.

		Mean diameter (cm)	Mean height (m)	Dominant height (m)
Zone 1	Av. value	23.6	17.7	20.5
	St. dev	± 2.7	± 0.9	± 2.2
	Minimum	19.4	16.2	16.4
	Maximum	28.2	19.2	24.7

### Tree network construction

To characterize spatial patterns of individual-level competitions, all trees present within the forest plot were regarded as nodes<sup>16</sup>. We then defined three types of tree networks: (1) Competition for space (CS). In this network, trees were connected if the pairwise distance was less than 10m, which was an empirical extend of tree interactions; (2) Competition for light (CL). Trees in this network were connected only if they were overlapped. We used tree crown model proposed by Wang et al<sup>46</sup> to characterize tree crown

competition and define overlapping trees. In this model, a tree crown was considered as a disk (called “buffer region”) specified with radii  $R_i$  and treetop points  $P_i$ . Two tree crowns, Tree-1 and Tree-2 with treetop points  $P_1$  and  $P_2$ , were separated if the geographic distance between two treetop points is large than the sum of radii of Tree-1 and Tree-2 (i.e.  $\|P_1 - P_2\| > R_1 + R_2$ ). On the contrary, trees were overlapped if  $\|P_1 - P_2\| < R_1 + R_2$ ; (3) Weighted competition for light (WCL). The definition of overlapping trees was consisting with CL. In WCL, however, each edge was assigned by a value, which indicated the intensity of tree crown competition. In the case of two individual trees, we assumed that the intensity of competition for light was proportional to the crown sizes as:

$$CI_{ij} = \frac{1}{R_{ij}} \frac{R_j}{R_i} \quad (1)$$

where  $CI_{ij}$  is the competition index between the overlapped  $i$ -th and  $j$ -th tree crown;  $R_i$  and  $R_j$  are the radii of the “buffer” regions of  $i$ -th and  $j$ -th tree crowns;  $R_{ij}$  is the line segment between  $P_1$  and  $P_2$  falling in “buffer” regions of both trees, which computed as<sup>46</sup>

$$R_{ij} = (R_i + R_j) - \|P_i - P_j\| \quad (2)$$

Obviously, competition effect caused by  $i$ -th to  $j$ -th tree ( $CI_{ij}$ ) was not equal to that cause by  $j$ -th to  $i$ -th tree ( $CI_{ji}$ ). Hence WCL was a directed and weighted tree network while CS and CL were undirected tree networks.

### Spatial null model generation

To validate three types of tree networks, we used various types of spatial null models based on different ecological hypotheses (Fig. 1). We first tested the hypothesis of complete spatial randomness (CSR) and random labelling (RL) (i.e.  $R_i$  was assigned by random values). We performed 199 Monte Carlo simulations of CSR-RL and generated tree network characteristics.

As an alternative model to CSR, we used cluster process model to simulate dispersal limitation hypothesis. We designated a 200m×200m survey area for model generation. A cluster process first generates parent points with intensity  $\kappa$ , and then each parent points give rise to a Poisson number ( $\mu$ ) of offspring points, independently distributed in a circular area of radius  $R$  centered at the parent (Wiegand & Moloney 2013; Baddeley et al., 2016). The probability density of distance from parent point to offspring (i.e. dispersal kernels) varies among specific cluster models. In a Matérn process, offspring points are uniformly distributed in the disc. In Thomas process, the displacement vector follows a Gaussian distribution. The intensity of parent points  $\kappa$ , the average number of the offspring for each parents  $\mu$ , and the radius of dispersal area  $R$  were set as 0.015, 3, and 5m, respectively. Then we assign a value to each tree generated by the model as the canopy radius, range from 2–5m.

To simulate competition exclusion hypothesis, we chose Gibbs process model. A Gibbs process model assumes that interactions occur between the points. It first generates many realizations of CSR, and deletes any realizations does not follow the specific rules. In Gibbs hard core (HC) process, any realizations that contain points closed to a distance of  $R$  would be deleted. In Strass process, however, the probability of removing realizations that violate this constraint  $p$  ranges from 0–1 (Baddeley et al., 2016). Here, we set  $p$  as 0.5,  $R$  as 4m. The intensity of points  $\kappa$  is 0.015.

## Tree spatial patterns and interactions characterization

To explore spatial patterns of tree interactions, we used several spatial explicit metrics (Fig. 1). For network analyses, we computed four types of network characteristics, namely the density  $D$  of the network, the average node degree  $k$ , the average path length  $L$ , and the clustering coefficient  $C^{16}$ . We further performed spline interpolation to analyze spatial distribution of node degree and betweenness centrality of all nodes in the network.

As an alternative method to network analyses, we performed spatial point pattern analysis<sup>26,29,40,47</sup> to characterize tree spatial patterns.  $K(r)$  and  $g(r)$  were chosen to describe the second-order point pattern. Second-order spatial patterns corresponds to aggregated [ $g(r) > 1$ ], random [ $g(r) = 1$ ], or regular distribution [ $g(r) < 1$ ]<sup>24</sup>. Given the null hypothesis of CSR, a total of 199 Monte-Carlo simulations were performed, generating a confidence envelope to describe the maximum and minimum values of simulated results. Spatial point pattern analysis was conducted using the ‘spatstat’ package<sup>26</sup> in R software, version 4.0.2.

## Declarations

## Data availability

The datasets used for our case study can be obtained in the study by Cantiani & Marchi (<https://zenodo.org/record/438681#.YiXTRHxByho>), and the associated metadata can be found at <https://metadata-afs.nancy.inra.fr/geonetwork/srv/eng/catalog.search#/metadata/73591027-0f1e-40a3-95d0-b614517c1290>. All data and codes generated during our simulated study are included in the Supplementary Information files.

## Code availability

Code of the simulation study is available from the corresponding author upon request.

## Author contributions statement

H.W. designed the study. C.P. wrote the code and performed analyses. M.C. supervised the research. H.W., C.P., and M.C. discussed the results and wrote the manuscript.

# Additional information

Code of spatial null model simulation is available from the corresponding author upon request.

The authors declare no competing interests.

## References

1. Bonan, G. B. Forests and climate change: Forcings, feedbacks, and the climate benefits of forests. *Science* 320, 1444–1449, DOI: <https://doi.org/10.1126/science.1155121> (2008).
2. Le Quere, C. *et al.* Global Carbon Budget 2016. *Earth Syst. Sci. Data* 8, 605–649, DOI: <https://doi.org/10.5194/essd-8-605-2016> (2016).
3. Mi, X. *et al.* The global significance of biodiversity science in China: an overview. *Natl. Sci. Rev.* 8, DOI: <https://doi.org/10.1093/nsr/nwab032> (2021).
4. Kauppi, P. E., Sandstrom, V. & Lipponen, A. Forest resources of nations in relation to human well-being. *Plos One* 13, DOI: <https://doi.org/10.1371/journal.pone.0196248> (2018).
5. Anderegg, W. R. L. *et al.* Climate-driven risks to the climate mitigation potential of forests. *Science* 368, eaaz7005, DOI: <https://doi.org/10.1126/science.aaz7005> (2020).
6. Haddad, N. M. *et al.* Habitat fragmentation and its lasting impact on Earth's ecosystems. *Sci. Adv.* 1, DOI: <https://doi.org/10.1126/sciadv.1500052> (2015).
7. Wilson, M. C. *et al.* Habitat fragmentation and biodiversity conservation: key findings and future challenges. *Landscape Ecol.* 31, 219–227, DOI: <https://doi.org/10.1007/s10980-015-0312-3> (2016).
8. Holl, K. D. Restoring tropical forests from the bottom up. *Science* 355, 455–456, DOI: <https://doi.org/10.1126/science.aam5432> (2017).
9. Audino, L. D., Murphy, S. J., Zambaldi, L., Louzada, J. & Comita, L. S. Drivers of community assembly in tropical forest restoration sites: role of local environment, landscape, and space. *Ecol. Appl.* 27, 1731–1745, DOI: <https://doi.org/10.1002/eap.1562> (2017).
10. Temperton, V. M., Hobbs, R. J., Nuttle, T. & Halle, S. in *Assembly rules and restoration ecology: bridging the gap between theory and practice. [Science and Practice of Ecological Restoration.]* 1–439 (2004).
11. Young, T. P., Chase, J. M. & Huddleston, R. T. Community succession and assembly: comparing, contrasting and combining paradigms in the context of ecological restoration. *Ecol. Restor.* 19, 5–18, DOI: <https://doi.org/10.3368/er.19.1.5> (2001).
12. Vellend, M. *The Theory of Ecological Communities*. (Princeton University Press, 2016).
13. HilleRisLambers, J., Adler, P. B., Harpole, W. S., Levine, J. M. & Mayfield, M. M. Rethinking Community Assembly through the Lens of Coexistence Theory. *Annu. Rev. Ecol. Evol. S.* 43, 227–248, DOI: <https://doi.org/10.1146/annurev-ecolsys-110411-160411> (2012).

14. Connell, J. H. On the Role of Natural Enemies in Preventing Competitive Exclusion in Some Marine Animals and in Rain Forest Trees. In: Den Boer, P.J. and Gradwell, G.R., Eds., *Dynamics of Populations*, Centre for Agricultural Publishing and Documentation, Wageningen, The Netherlands (1971).
15. Janzen, D. H. Herbivores and the Number of Tree Species in Tropical Forests. *Am. Nat.* 104, 501–528, DOI: <https://doi.org/10.1086/282687> (1970).
16. Schmid, J. S., Taubert, F., Wiegand, T., Sun, I. F. & Huth, A. Network science applied to forest megaplots: tropical tree species coexist in small-world networks. *Sci. Rep.* 10, DOI: <https://doi.org/10.1038/s41598-020-70052-8> (2020).
17. Wang, H. X. *et al.* Prevalence of Inter-Tree Competition and Its Role in Shaping the Community Structure of a Natural Mongolian Scots Pine (*Pinus sylvestris* var. *mongolica*) Forest. *Forests* 8, DOI: <https://doi.org/10.3390/f8030084> (2017).
18. Hubbell, S. P. *et al.* Light-gap disturbances, recruitment limitation, and tree diversity in a neotropical forest. *Science* 283, 554–557, DOI: <https://doi.org/10.1126/science.283.5401.554> (1999).
19. Janik, D. *et al.* Breaking through beech: A three-decade rise of sycamore in old-growth European forest. *Forest Ecol. Manag.* 366, 106117, DOI: <https://doi.org/10.1016/j.foreco.2016.02.003> (2016).
20. Svatek, M., Rejzek, M., Kvasnica, J., Repka, R. & Matula, R. Frequent fires control tree spatial pattern, mortality and regeneration in Argentine open woodlands. *Forest Ecol. Manag.* 408, 129–136, DOI: <https://doi.org/10.1016/j.foreco.2017.10.048> (2018).
21. Giammarchi, F. *et al.* Effects of the lack of forest management on spatiotemporal dynamics of a subalpine *Pinus cembra* forest. *Scand. J. Forest. Res.* 32, 142–153, DOI: <https://doi.org/10.1080/02827581.2016.1207802> (2017).
22. Janik, D. *et al.* Patterns of *Fraxinus angustifolia* in an alluvial old-growth forest after declines in flooding events. *Eur. J. Forest Res.* 135, 215–28, DOI: <https://doi.org/10.1007/s10342-015-0925-8> (2016).
23. Bagchi, R. *et al.* Defaunation increases the spatial clustering of lowland Western Amazonian tree communities. *J. Ecol.* 106, 1470–1482, DOI: <https://doi.org/10.1111/1365-2745.12929> (2018).
24. Obiang, N. L. E. *et al.* Determinants of spatial patterns of canopy tree species in a tropical evergreen forest in Gabon. *J. Veg. Sci.* 30, 929–939, DOI: <https://doi.org/10.1111/jvs.12778> (2019).
25. Zhang, L. Y., Dong, L. B., Liu, Q. & Liu, Z. G. Spatial Patterns and Interspecific Associations During Natural Regeneration in Three Types of Secondary Forest in the Central Part of the Greater Khingan Mountains, Heilongjiang Province, China. *Forests* 11, DOI: <https://doi.org/10.3390/f11020152> (2020).
26. Baddeley, A., Rubak, R. & Turner, R. *Spatial point patterns, methodology and applications with R*. (CRC Press, 2016).
27. Gabriel, E. Spatial Point Patterns: Methodology and Applications with R. *Math. Geosci.* 49, 815–817, DOI: <https://doi.org/10.1007/s11004-016-9670-x> (2017).

28. Wiegand, T. & Moloney, K. A. Rings, circles, and null-models for point pattern analysis in ecology. *Oikos* 104, 209–229, DOI: <https://doi.org/10.1111/j.0030-1299.2004.12497.x> (2004).
29. Wiegand, T. *et al.* Spatially Explicit Metrics of Species Diversity, Functional Diversity, and Phylogenetic Diversity: Insights into Plant Community Assembly Processes. *Annu. Rev. Ecol. Evol. S.* 48, 329–351, DOI: <https://doi.org/10.1146/annurev-ecolsys-110316-022936> (2017).
30. Plotkin, J. B., Chave, J. M. & Ashton, P. S. Cluster analysis of spatial patterns in Malaysian tree species. *Am. Nat.* 160, 629-644, DOI: <https://doi.org/10.1086/342823> (2002).
31. Ripley, B. D. 2nd-Order Analysis of Stationary Point Processes. *J. Appl. Probab.* 13, 255–266, DOI: <https://doi.org/10.2307/3212829> (1976).
32. Diggle, P. *Statistical analysis of spatial point patterns*. (Academic Press, 1983).
33. He, F. L. & Gaston, K. J. Estimating species abundance from occurrence. *Am. Nat.* 156, 553–559, DOI: <https://doi.org/10.1086/303403> (2000).
34. Pielou, E. C. The Use of Point-To-Plant Distances in the Study of the Pattern of Plant-Populations. *J. Ecol.* 47, 607–613, DOI: <https://doi.org/10.2307/2257293> (1959).
35. Fuller, M. M., Wagner, A. & Enquist, B. J. Using network analysis to characterize forest structure. *Nat. Resour. Model.* 21, 225–247, DOI: <https://doi.org/10.1111/j.1939-7445.2008.00004.x> (2008).
36. Losapio, G., Montesinos-Navarro, A. & Saiz, H. Perspectives for ecological networks in plant ecology. *Plant. Ecol. Divers.* 12, 87–102, DOI: <https://doi.org/10.1080/17550874.2019.1626509> (2019).
37. Montoya, J. M., Pimm, S. L. & Sole, R. V. Ecological networks and their fragility. *Nature* 442, 259-264, DOI: <https://doi.org/10.1038/nature04927> (2006).
38. Proulx, S. R., Promislow, D. E. L. & Phillips, P. C. Network thinking in ecology and evolution. *Trends. Ecol. Evol.* 20, 345-353, DOI: <https://doi.org/10.1016/j.tree.2005.04.004> (2005).
39. Nakagawa, Y., Yokozaw, M. & Hara, T. Complex network analysis reveals novel essential properties of competition among individuals in an even-aged plant population. *Ecol. Complex.* 26, 95-116, DOI: <https://doi.org/10.1016/j.ecocom.2016.03.005> (2016).
40. Wiegand, T. & Moloney, K. A. *Handbook of spatial point pattern analysis in ecology*. (CRC Press, 2013).
41. Barthelemy, M. Spatial networks. *Phys. Rep.* 499, 1–101, DOI: <https://doi.org/10.1016/j.physrep.2010.11.002> (2011).
42. Zhang, G. Q. *et al.* Designing near-natural planting patterns for plantation forests in China. *For. Ecosyst.* 6, DOI: <https://doi.org/10.1186/s40663-019-0187-x> (2019).
43. Martinez-Lopez, V., Garcia, C., Zapata, V., Robledano, F. & De la Rúa, P. Intercontinental long-distance seed dispersal across the Mediterranean Basin explains population genetic structure of a bird-dispersed shrub. *Mol. Ecol.* 29, 1408–1420, DOI: <https://doi.org/10.1111/mec.15413> (2020).
44. Dale, M. R. T. & Fortin, M. J. From Graphs to Spatial Graphs. *Annu. Rev. Ecol. Evol. S.* 41, 21–38, DOI: <https://doi.org/10.1146/annurev-ecolsys-102209-144718> (2010).

45. Cantiani, P. & Marchi, M. A spatial dataset of forest mensuration collected in black pine plantations in central Italy. *Ann. Forest. Sci.* 74, DOI: <https://doi.org/10.1007/s13595-017-0648-8> (2017).
46. Wang, X. F., Zheng, G., Yun, Z. X. & Moskal, L. M. Characterizing Tree Spatial Distribution Patterns Using Discrete Aerial Lidar Data. *Remote. Sens.* 12, DOI: <https://doi.org/10.3390/rs12040712> (2020).
47. Cressie Noel, A. C. *Statistics for spatial data.* (Wiley-Interscience, 1993).

## Figures

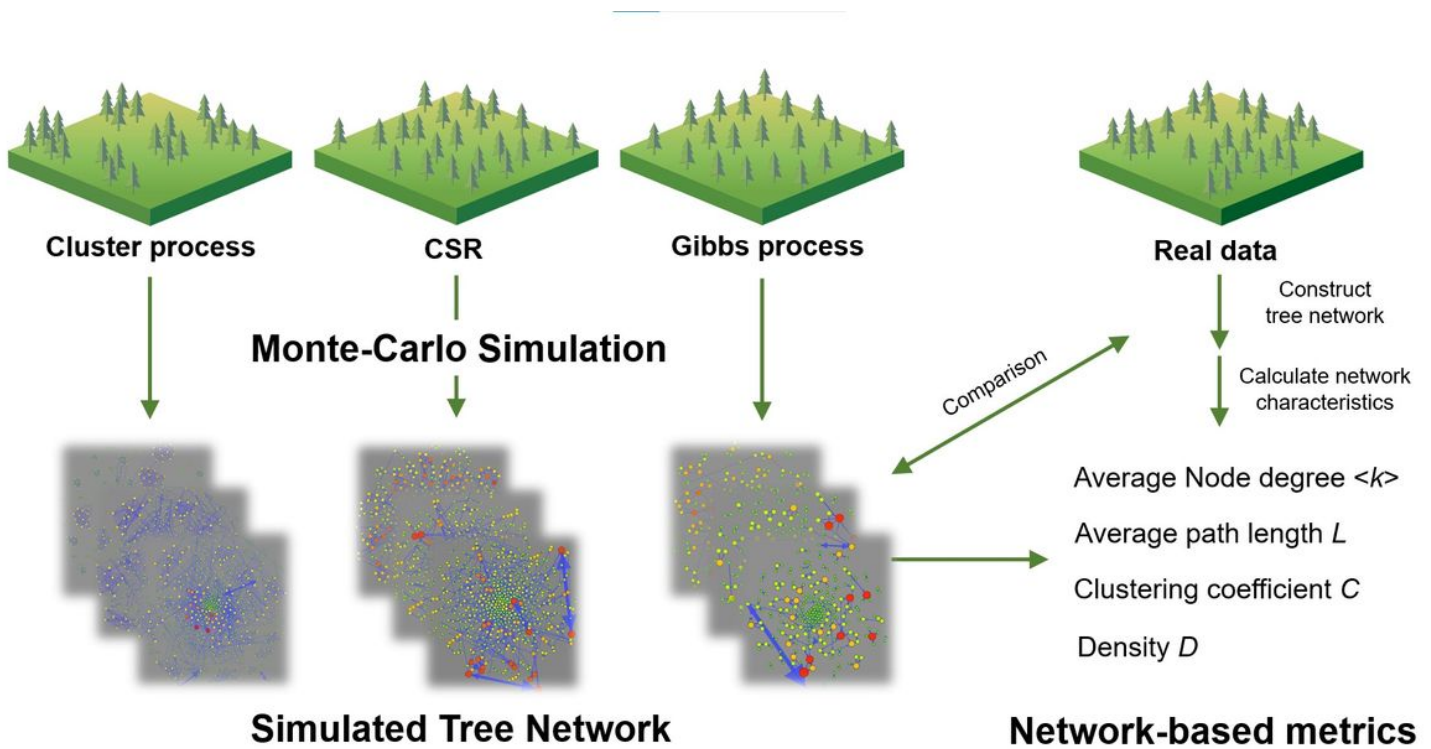


**Figure 1**

Overview of procedure using network characteristics to examine spatial patterns of tree competition. Monte-Carlo simulations of various spatial null models should be carried out to translate ecological processes into corresponding patterns. Network-based metrics are then calculated for each realization of simulation. Metrics that fail to distinguish different processes should be discarded. The last step is to perform network analysis based on empirical data and make comparisons between empirical and simulated results.

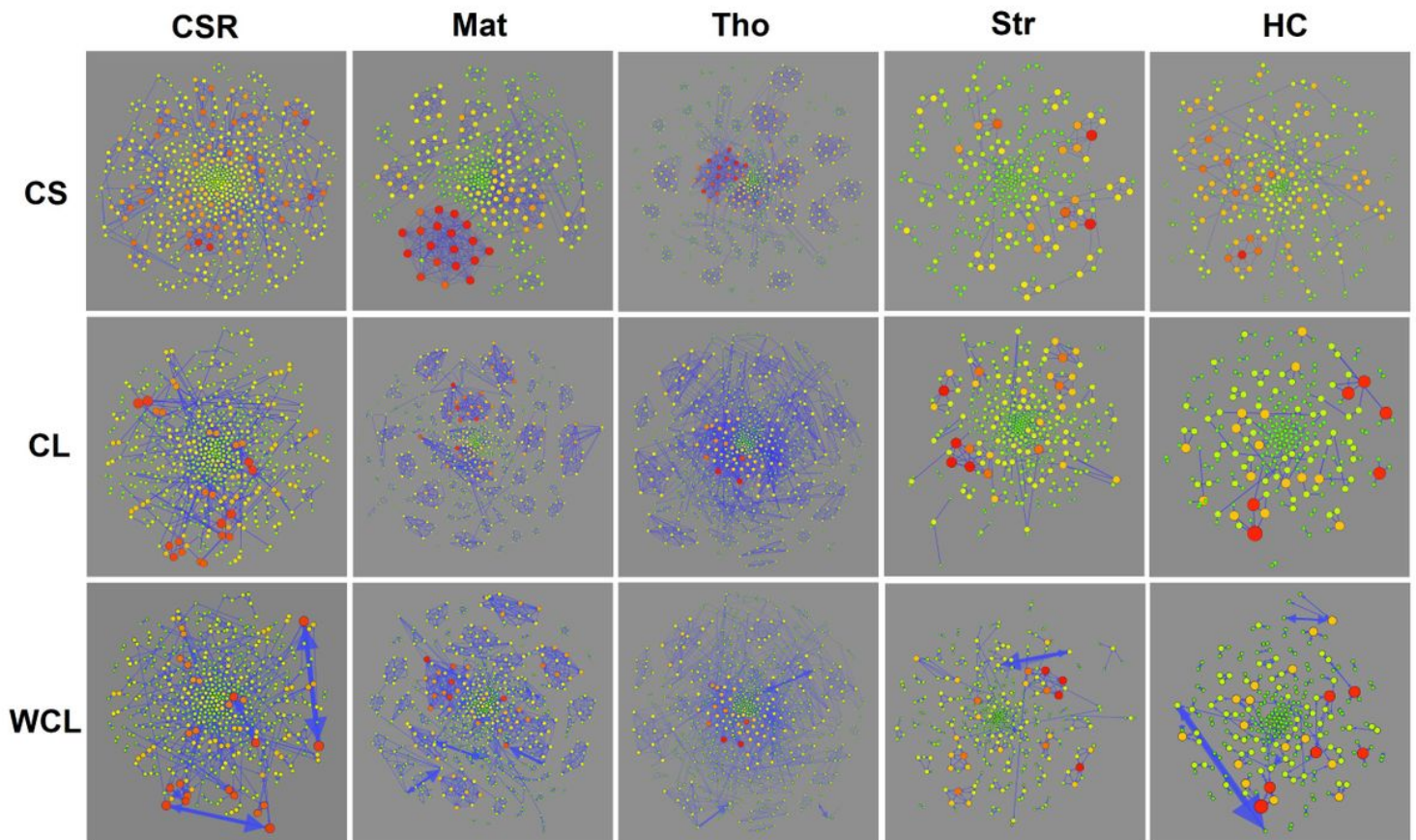


**Figure 2**

Three types of the networks (Competition for space, CS; Competition for light, CL; weighted competition for light, WCL) for each spatial null model. Each node represents a tree, and each edge reflects competition. The size and color of the node reflect the degree of the node, the redder nodes have greater degree. The networks are drawn using Gephi 0.9.2 with a layout of ForceAtlas2. In WCL, the weight is proportional to the size of the edges. Arrow size reflects the intensity of asymmetric competition.

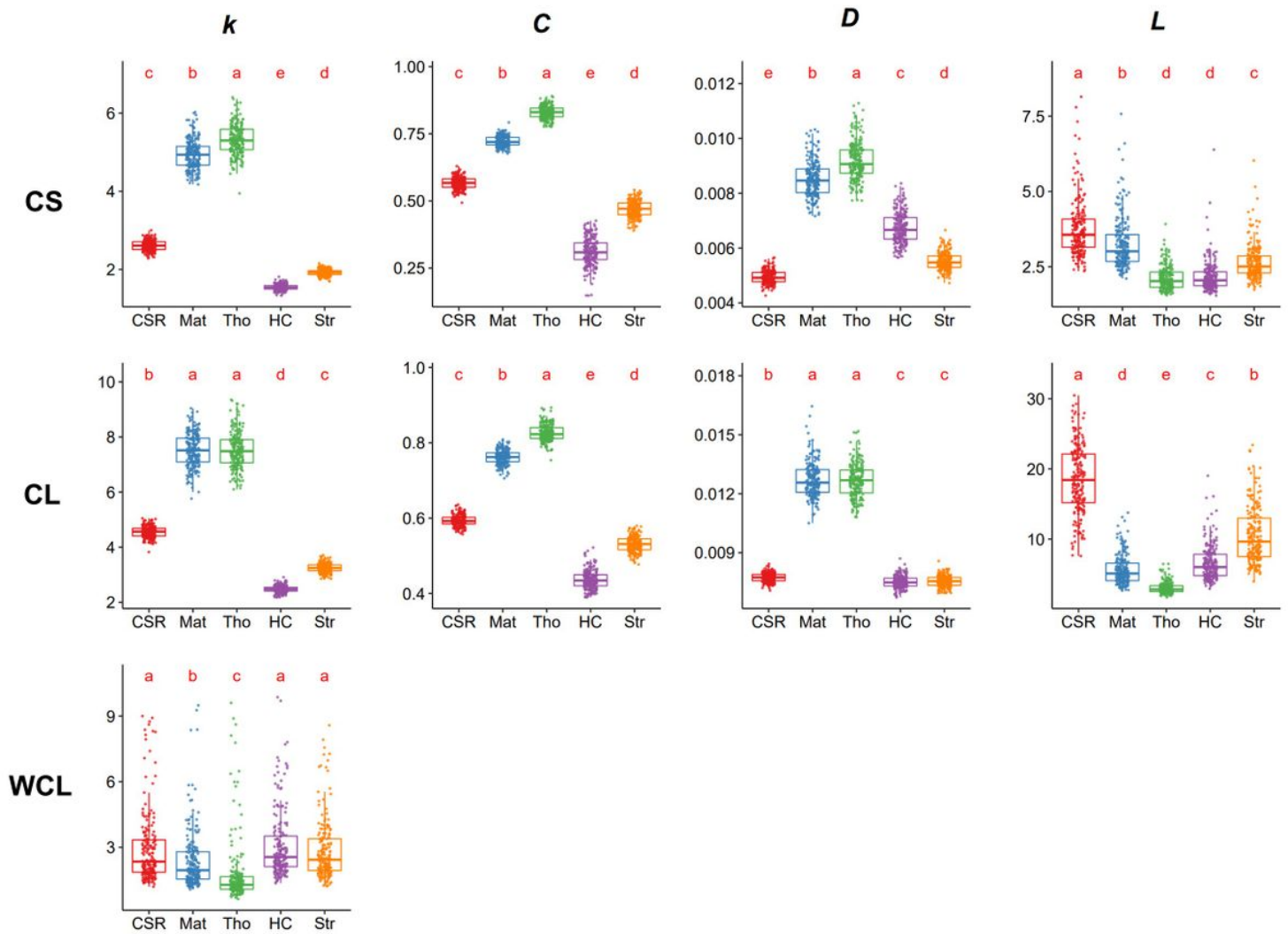
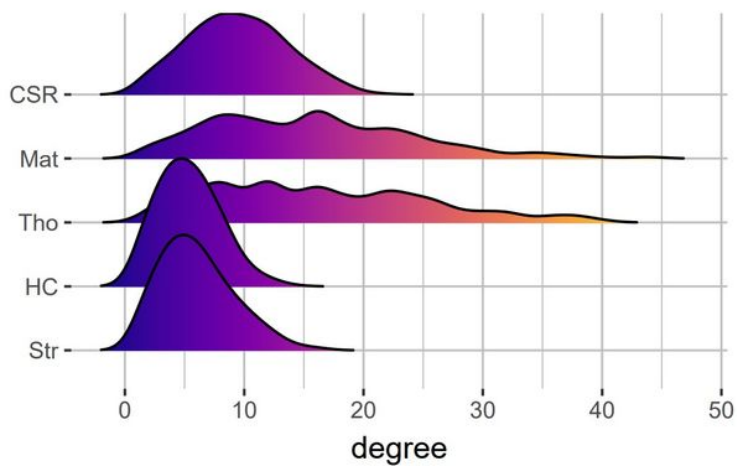


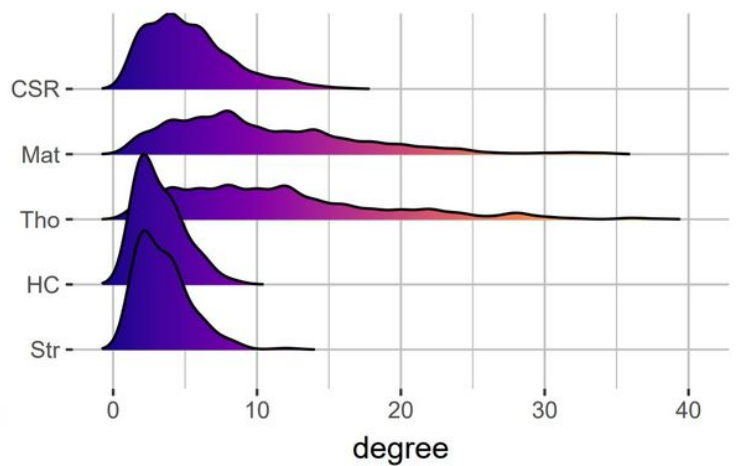
**Figure 3**

Basic characteristics of tree types of the tree networks based on five spatial null models (Complete spatial randomness, CSR; Matérn process, Mat; Thomas process, Tho; Gibbs hard core process, HC; Strass process, Str). Values of each characteristic are generated by 199 Monte-Carlo simulations. the average node degree  $k$ , the clustering coefficient  $C$ , the density  $D$ , the average path length  $L$ . Differences among five models were examined by ANOVA, followed by a Tukey multiple comparisons posttest. In WCL, the weighted average node degree  $k$  was calculated, while values of  $C$ ,  $D$ , and  $L$  are consistent with that of CL due to ignorance of edge weight information.

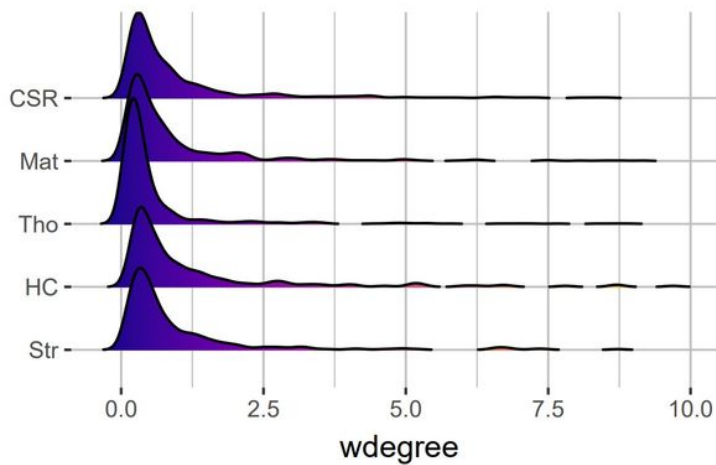
**a** CS distribution of degrees



**b** CL distribution of degrees



**c** WCL distribution of degrees



**d** WCL distribution of  $Cl_{ij}$

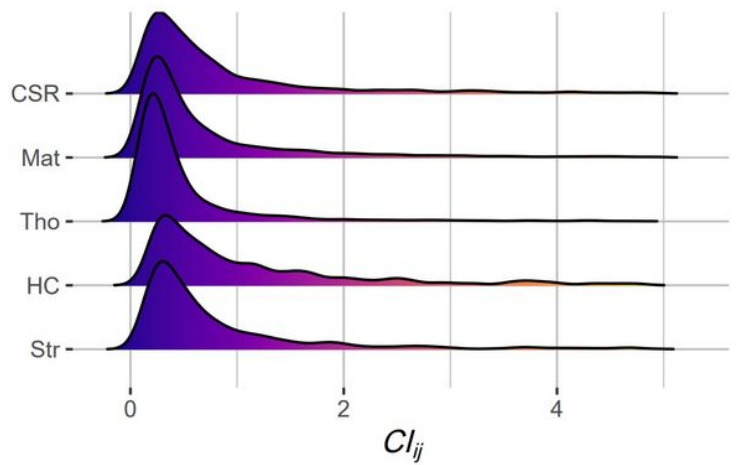


**Figure 4**

Node degree distribution and edge distribution of the tree network. **(a, b)** The node degree distribution of CS and CL networks based on five spatial null models. **(c)** The weighted degree distribution of WCL. **(d)** Distribution of edge weight (namely  $Cl_{ij}$ ) in WCL.

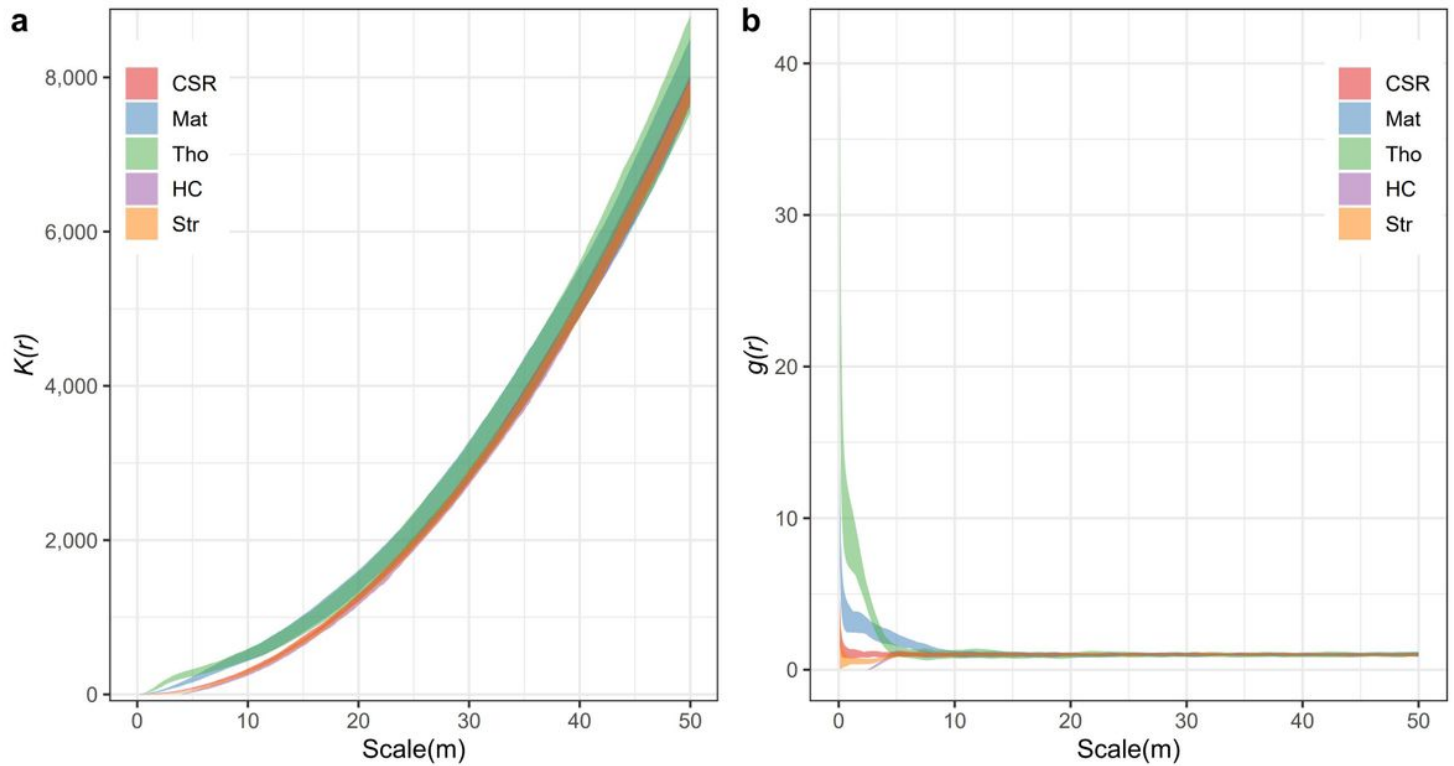


**Figure 5**

Variations of univariate  $K(r)$  and  $g(r)$  functions based on five spatial null models generated by 199 Monte-Carlo simulations. **(a)**  $K(r)$  function. **(b)**  $g(r)$  function. Boundary of envelopes reflects the maximum and minimum values of  $K(r)$  and  $g(r)$  functions in the simulations, colorful areas show the 95% confidence limits around the predicted  $K(r)$  or  $g(r)$  estimated from 199 random simulations of the point process

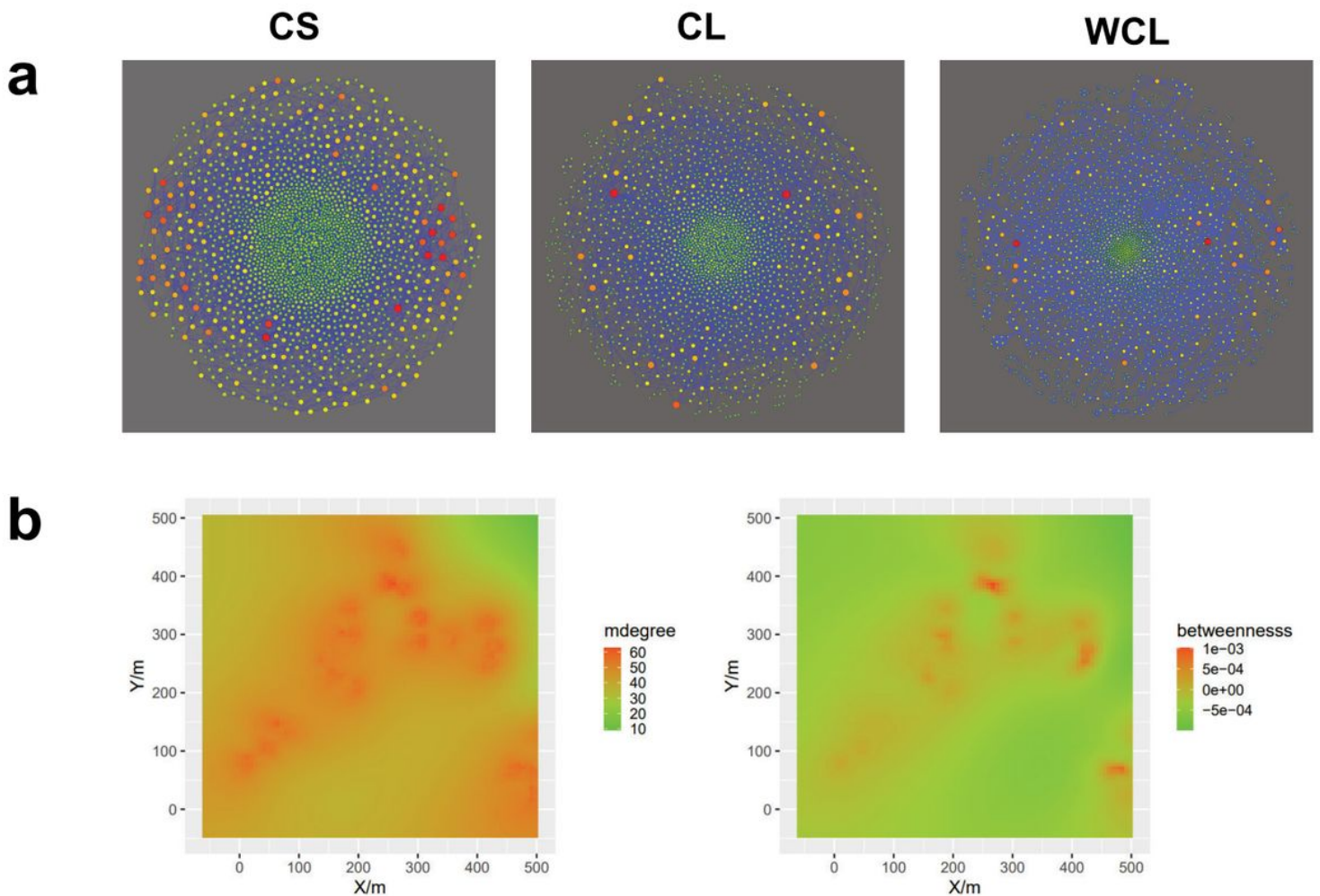


**Figure 6**

(a) Three types of the networks (Competition for space, CS; Competition for light, CL; weighted competition for light, WCL) based on Tuscany dataset. Each node represents a tree, and each edge reflects competition. The size and color of the node reflect the degree of the node, the redder nodes have greater degree. In WCL, the weight is proportional to the size of the edges. (b) Distribution of node attributes generated by spline interpolation based on CS network of the Tuscany dataset. The depth of the color is corresponding to the values of node attributes.

## Supplementary Files

This is a list of supplementary files associated with this preprint. Click to download.

- [RethinkNet.SupplementaryFigureandTable.pdf](#)
- [RethinkNet.simudata.xlsx](#)